



AFRL-RY-WP-TP-2010-1250

GAIN COUPLING OF CLASS A SEMICONDUCTOR LASERS (POSTPRINT)

Chris Hessenius, Mahmoud Fallahi, and Jerome Moloney

University of Arizona

Nathan Terry and Robert Bedford

Electro Optic Components Branch

Aerospace Components and Subsystems Technology Division

SEPTEMBER 2010

Approved for public release; distribution unlimited.

See additional restrictions described on inside pages

STINFO COPY

© 2010 Optical Society of America

**AIR FORCE RESEARCH LABORATORY
SENSORS DIRECTORATE
WRIGHT-PATTERSON AIR FORCE BASE, OH 45433-7320
AIR FORCE MATERIEL COMMAND
UNITED STATES AIR FORCE**

REPORT DOCUMENTATION PAGE					<i>Form Approved</i> OMB No. 0704-0188	
The public reporting burden for this collection of information is estimated to average 1 hour per response, including the time for reviewing instructions, searching existing data sources, gathering and maintaining the data needed, and completing and reviewing the collection of information. Send comments regarding this burden estimate or any other aspect of this collection of information, including suggestions for reducing this burden, to Department of Defense, Washington Headquarters Services, Directorate for Information Operations and Reports (0704-0188), 1215 Jefferson Davis Highway, Suite 1204, Arlington, VA 22202-4302. Respondents should be aware that notwithstanding any other provision of law, no person shall be subject to any penalty for failing to comply with a collection of information if it does not display a currently valid OMB control number. PLEASE DO NOT RETURN YOUR FORM TO THE ABOVE ADDRESS.						
1. REPORT DATE (DD-MM-YY) September 2010		2. REPORT TYPE Journal Article Postprint		3. DATES COVERED (From - To) 13 January 2010 – 01 June 2010		
4. TITLE AND SUBTITLE GAIN COUPLING OF CLASS A SEMICONDUCTOR LASERS (POSTPRINT)				5a. CONTRACT NUMBER In-house		
				5b. GRANT NUMBER		
				5c. PROGRAM ELEMENT NUMBER 62204F		
6. AUTHOR(S) Chris Hessenius, Mahmoud Fallahi, and Jerome Moloney (University of Arizona) Nathan Terry and Robert Bedford (AFRL/RYPD)				5d. PROJECT NUMBER 2002		
				5e. TASK NUMBER IH		
				5f. WORK UNIT NUMBER 2002IH0E		
7. PERFORMING ORGANIZATION NAME(S) AND ADDRESS(ES) University of Arizona Arizona Center for Mathematical Sciences Tucson, AZ 85721				8. PERFORMING ORGANIZATION REPORT NUMBER AFRL-RY-WP-TP-2010-1250		
Electro Optic Components Branch (AFRL/RYPD) Aerospace Components and Subsystems Technology Division Air Force Research Laboratory Sensors Directorate Wright-Patterson Air Force Base, OH 45433-7320 Air Force Materiel Command, United States Air Force						
9. SPONSORING/MONITORING AGENCY NAME(S) AND ADDRESS(ES) Air Force Research Laboratory Sensors Directorate Wright-Patterson Air Force Base, OH 45433-7320 Air Force Materiel Command United States Air Force				10. SPONSORING/MONITORING AGENCY ACRONYM(S) AFRL/RYPD		
				11. SPONSORING/MONITORING AGENCY REPORT NUMBER(S) AFRL-RY-WP-TP-2010-1250		
12. DISTRIBUTION/AVAILABILITY STATEMENT Approved for public release; distribution unlimited.						
13. SUPPLEMENTARY NOTES Journal article published in <i>Optics Letters</i> , Vol. 35, No. 18, September 15, 2010. PAO Case Number: 88ABW-10-3291; Clearance Date: 16 Jun 2010. Paper contains color. © 2010 Optical Society of America. The U.S. Government is joint author of the work and has the right to use, modify, reproduce, release, perform, display, or disclose the work.						
14. ABSTRACT We report on the development of a gain-coupled class A semiconductor laser for dual-wavelength generation via optical switching. A vertical external cavity surface emitting laser (VECSEL) structure is used, because it provides a flexible platform for high-power, high-brightness output in the near-IR and visible ranges. For the first time (to our knowledge), two VECSEL cavities sharing a common gain region are studied. Because the cavities are in competition for common carriers, birefringent filters in the external cavity control the laser cavity thresholds; this configuration demonstrates the possibility of switching between the two cavities, which can operate at different wavelengths. However, in this Letter we also show, numerically and experimentally, that with the consideration of spontaneous emission, it is possible to maintain simultaneous lasing in each cavity at a different wavelength.						
15. SUBJECT TERMS lasers, semiconductor						
16. SECURITY CLASSIFICATION OF:			17. LIMITATION OF ABSTRACT: SAR	18. NUMBER OF PAGES 10	19a. NAME OF RESPONSIBLE PERSON (Monitor) Robert G. Bedford 19b. TELEPHONE NUMBER (Include Area Code) N/A	
a. REPORT Unclassified	b. ABSTRACT Unclassified	c. THIS PAGE Unclassified				

Gain coupling of class A semiconductor lasers

Chris Hassenius,^{1,*} Nathan Terry,² Mahmoud Fallahi,¹ Jerome Moloney,¹ and Robert Bedford²

¹College of Optical Sciences, University of Arizona, 1630 East University Boulevard, Tucson, Arizona 85721, USA

²Sensors Directorate, Air Force Research Laboratory Wright-Patterson Air Force Base, Ohio 45433, USA

*Corresponding author: chassenius@optics.arizona.edu

Received June 17, 2010; revised August 9, 2010; accepted August 17, 2010;
posted August 19, 2010 (Doc. ID 130280); published September 7, 2010

We report on the development of a gain-coupled class A semiconductor laser for dual-wavelength generation via optical switching. A vertical external cavity surface emitting laser (VECSEL) structure is used, because it provides a flexible platform for high-power, high-brightness output in the near-IR and visible ranges. For the first time (to our knowledge), two VECSEL cavities sharing a common gain region are studied. Because the cavities are in competition for common carriers, birefringent filters in the external cavity control the laser cavity thresholds; this configuration demonstrates the possibility of switching between the two cavities, which can operate at different wavelengths. However, in this Letter we also show, numerically and experimentally, that with the consideration of spontaneous emission, it is possible to maintain simultaneous lasing in each cavity at a different wavelength. © 2010 Optical Society of America

OCIS codes: 140.3325, 140.5960, 140.7260.

High-power semiconductor lasers with wavelength switching capability are of great interest in a range of applications including optical communication. Optically pumped vertical external cavity surface emitting lasers (VECSELs) have proven to be very reliable in achieving multiwatt high-brightness emission [1–3]. The insertion of a birefringent filter (BF) in a VECSEL cavity allows a narrow-linewidth, widely tunable emission [2,4,5]. In this Letter we report gain coupling, switching, and dual-wavelength operation in VECSELs by combining a linear and a v-shaped cavity VECSEL sharing the same gain region. We present unique behaviors such as high-power optical switching and tunable dual-wavelength emission. Experimental results and supporting modeling results are reported.

The novel design, shown in Fig. 1, is the simplest dual-cavity gain-coupled configuration consisting of a linear cavity (cavity 1) and a v-shaped cavity (cavity 2) coupled by sharing a common VECSEL quantum-well gain material. This design is unique in that each cavity oscillates at its own frequency, while the BFs eliminate optical coupling between the laser cavities, which may occur due to scattering. Unlike other dual-wavelength VECSELs that employ a single external cavity with either quantum wells designed for different wavelengths [6] or polarization optics that split the mode into spatially separated regions on the gain chip [7,8], this configuration relies on the naturally broad semiconductor gain and provides control over each cavity independently. This dual-cavity design allows us to potentially avoid instabilities [9,10] due to photon interaction between the two cavities while maintaining the ability to simultaneously control the output of each.

The VECSEL gain chip used in the experiment is designed for emission around 975 nm. The active region consists of 14 InGaAs compressive strained quantum wells 8 nm thick surrounded by GaAsP strain compensation layers and AlGaAs pump-absorbing barriers. A 99.9% distributed Bragg reflector stack made of 25 pairs of $\text{Al}_{0.2}\text{Ga}_{0.8}\text{As}/\text{AlAs}$ is grown on the top of the active region, and a single-layer quarter-wave low-reflection

coating of SiO_2 is applied to the surface of the chip to enhance the 975 nm signal.

The geometry, cavity lengths, and reflectivities are shown in Fig. 1. The output power of cavity 1 can be controlled by rotating the BF in cavity 2, and vice versa. For example, if a constant pump power is maintained and the BF in cavity 1 remains fixed, tuning the BF in cavity 2 creates regions where only cavity 1 lases and regions where only cavity 2 lases. In this case, the lasing wavelength of cavity 1 is essentially constant at the wavelength selected by the BF in cavity 1.

A map of the output power for each cavity as a function of wavelength of each of the two cavities is shown in Fig. 2, as measured using a thermopile detector. Figure 2(a) shows the output power of cavity 1 over the entire tuning range of the chip, while Fig. 2(b) shows the output power of cavity 2. Figure 2 is given for a fixed pump power of ~ 15 W, and the two axes represent the tuning of each cavity with respect to the wavelength corresponding to minimum uncoupled cavity threshold. $\Delta\lambda_{1,2}$ are the offsets with respect to this minimum uncoupled threshold of each respective cavity.

Figure 2 shows there are broad operating regimes where either cavity 1 or cavity 2 is lasing. These regions result directly from gain competition between the two cavities. By adjusting the BF we alter the resonant periodic mode overlap enhancement [11,12], which in turn

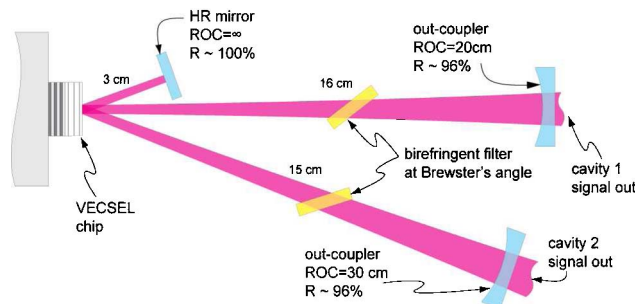


Fig. 1. (Color online) Schematic of coupled VECSEL system. The BFs are used to tune each cavity-respective wavelength within the semiconductor gain bandwidth. The linear cavity (cavity 1) passes once through the chip in a round trip, while the v-shaped cavity (cavity 2) passes twice.

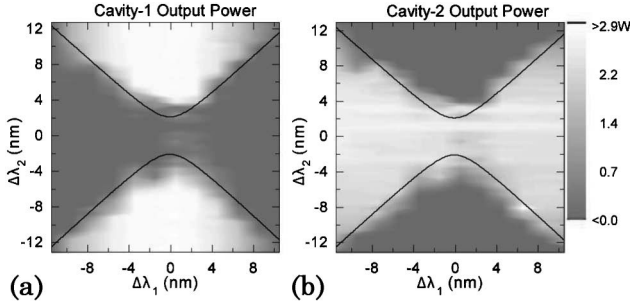


Fig. 2. Map of the output power for each cavity as a function of the wavelength with (a) the linear cavity (1) and (b) the v-shaped cavity (2) for cavity wavelengths at a fixed pump power of ~ 15 W. Gray-scale changes from completely off (dark), to completely on (light). The lines in (a) and (b) show the positions of the equal uncoupled threshold, indicating areas where both cavities operate simultaneously. $\Delta\lambda_{1,2}$ is the offset with respect to the wavelength of the minimum uncoupled threshold.

controls the threshold of the uncoupled cavities. We experimentally confirm this by measuring the threshold of each uncoupled cavity individually as a function of wavelength. Because the gain essentially “clamps” at threshold, the laser with the lowest threshold lases first, thereby inhibiting the ability of the other cavity to reach the threshold. By comparing the values of the threshold for each uncoupled cavity, we plot the regions of equal threshold where the laser switches from one cavity output to the other. For most operating regimes, the relative threshold of the uncoupled cavities is sufficient to indicate which of the two laser cavities will be on when the two cavities are coupled together. The boundary between each cavity lasing occurs where the uncoupled cavity thresholds are equal.

To understand this laser system, we first introduce a set of simplified rate equations, ignoring barrier absorption and spontaneous emission, patterned after a single-cavity case [13]:

$$\frac{dN}{dt} = \frac{P\Omega}{V_a \hbar \omega_p} - \frac{N}{\tau} - v_g g [\Gamma_{r1} S_1 + 2\Gamma_{r2} S_2], \quad (1)$$

$$\frac{dS_1}{dt} = -\frac{S_1}{\tau_{p1}} + v_g \Gamma_{1g} S_1, \quad (2)$$

$$\frac{dS_2}{dt} = -\frac{S_2}{\tau_{p2}} + 2v_g \Gamma_{2g} S_2. \quad (3)$$

In Eqs. (1)–(3), N is the carrier density, $S_{1,2}$ are the photon densities in the linear and the v cavities (1 and 2, respectively), P is the incident pump power, Ω is the pump absorption efficiency, ω_p is the angular frequency of the pump, τ is the carrier lifetime, v_g is the group velocity, $\Gamma_{r1,r2}$ is the resonant periodic gain enhancement factor in each cavity, g is the gain, $\tau_{p1,p2}$ are the photon lifetimes in each cavity, $\Gamma_{1,2}$ are the total overlap integrals, and V_a is the volume of the active region. The factor of 2 in front of the S_2 term in Eq. (1) accounts for the chip being a fold of the cavity; a round-trip of cavity 2 consists of twice the number of passes through the gain as cavity 1. There is no explicit photon coupling, so the

two cavities are solely coupled through the carrier density in the gain element.

We explain the cavity competition by analyzing the steady states of Eqs. (1)–(3). It becomes immediately evident that, for all cases where the uncoupled thresholds are not identical, either S_1 or S_2 will be zero. The cavity with the lowest losses lases first, preventing photons from building up in the other cavity. Fitting the threshold of cavity 1 without the influence of cavity 2 across the tuning range of the BF confirms this. We assume a logarithmic gain function $g(\lambda; N) = g_0 \ln(N/N_{tr}(\lambda))$, explicitly ignoring the shift-carrier density typically included [14]. In this case, the constant coefficient g_0 and the function $N_{tr}(\lambda)$, allowed to vary linearly with wavelength, are used as fitting parameters. This functional form was determined to be suitable over the tuning range and approximate carrier densities present in this laser system by using commercially available many-body software [15]. We then use these values to calculate the cavity 2 threshold over the same wavelength range. By comparing the predicted thresholds of the two cavities, we determine the boundaries indicated by the lines in Fig. 2.

Figure 2 and the description in the preceding paragraph explain the behavior of the coupled system everywhere except near the boundary when the BFs are tuned such that both uncoupled cavities have similar thresholds. In this boundary regime, a close inspection of Fig. 2 reveals regions where both S_1 and S_2 are nonzero, a scenario not predicted by solving Eqs. (1)–(3), except at the boundary $\frac{\Gamma_{12}}{\tau_{p1}} = \frac{\Gamma_{21}}{\tau_{p2}}$. This unstable point is not achievable in practice owing to noises in real systems. However, we see operating conditions near the boundary allow both lasers to be on, even at differences in wavelengths of 17 nm and 22 nm in the second and fourth quadrants of Fig. 2, respectively.

By chopping one of the cavities and using a 200 MHz detector, the temporal aspects of the switching action are observed. Figure 3(a) represents a region in Fig. 2, well away from the boundary, where cavity 1 is completely on and cavity 2 is completely off. We first block cavity 1, and then suddenly unblock the cavity, turning it on. Cavity 2 tends to zero symmetrically in this case, as the uncoupled threshold of cavity 1 is lower than that of the uncoupled cavity 2. Photons build up in cavity 1, dropping cavity 2

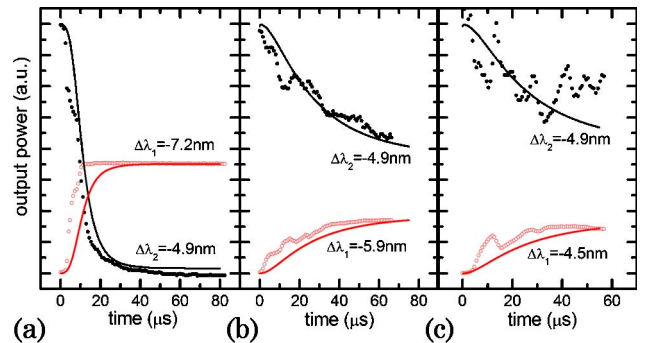


Fig. 3. (Color online) Plot of output power versus time for different cavity tunings. The linear cavity was chopped in the dual-cavity configuration. (a) Cavity tuned such that cavity switches from completely on to completely off. (b), (c) Various tuning such that the switching is less complete. Simulated results are shown as solid curves.

below the threshold; this result closely matches what is seen by chopping a single cavity. As we adjust the BF to tune closer to the regions of equal threshold, we see in Figs. 3(b) and 3(c) that the cavities begin to lase at the same time.

To account for the case of simultaneous lasing, the effect of spontaneous emission must be included in Eqs. (2) and (3) by appropriately adding a $\beta_{1,2}BN^2$ term, where B is the spontaneous emission coefficient and $\beta_{1,2}$ is the coupling of this emission to each cavity mode. When spontaneous emission is included, the gain coupling prevents one cavity from running away and the other from shutting off completely. Consider the case shown in Figs. 3(b) and 3(c), where cavities 1 and 2 are very near the areas of equal threshold. Cavity 1 begins blocked and is unblocked at time $t = 0$. The uncoupled threshold of cavity 1 is initially slightly lower, and the photon density increases at the expense of the photon density of cavity 2. As the photon density of cavity 2 drops, the relative contribution of the spontaneous emission increases. Because spontaneous emission is an additive term to the photon equation, it can be considered as a mechanism for reducing the threshold gain of cavity 2, thus lowering the uncoupled threshold of cavity 2 below that of cavity 1 and effectively reducing the photon density of cavity 1. This cycle is damped by the photon lifetime, allowing both cavities to operate simultaneously. This effective reduction in the threshold is, of course, very small, which is why this effect is important only when the two uncoupled thresholds are very close.

We confirm this effect by solving Eqs. (1)–(3) with the aforementioned spontaneous emission term included. In the model, we adjust $\Gamma_{r1,r2}$ in order to simulate the tuning of the BF. It takes less than a 1% change in the resonant periodic gain to account for the difference between Figs. 3(a) and 3(c). The calculated effect, shown as solid curves in Fig. 3, nicely predicts the overall shape of the curves. The experimental fluctuations seen in Figs. 3(b) and 3(c) are not fully understood, but they are believed to result from mechanical vibrations in the VECSEL experiment, which becomes very sensitive when the two cavities have nominally identical thresholds. Numerical investigations reveal that the switching time is primarily limited to the photon buildup of class A lasers [16], where the lifetime is a function of the sum of the uncoupled photon lifetimes.

The dual-cavity design allows for gain coupling of the VECSEL cavities. We examined the simplest case that employs a linear and a v cavity that are gain coupled. This coupling allows not only optical switching between two cavities operating at different wavelengths but also the simultaneous generation of different wavelengths from a common gain medium, at wavelengths anywhere near the boundary where the two laser thresholds are similar.

A fundamental set of rate equations is used to define an operation map where the areas of simultaneous operation and switching regions are plotted. We have numerically and experimentally identified and explained the boundary lines between linear and v-cavity dominance, defining the tuning capabilities of the dual-wavelength generation. In addition, it may be possible to expand the system to include several cavities centered on a common gain medium to allow for even more flexibility.

This work is supported by the United States Air Force Research Laboratory (USAFRL)/RY Director ER funds and the United States Air Force Office of Scientific Research (USAFOSR) lab task 08RY08COR. The authors would also like to acknowledge support from the National Science Foundation (NSF) and the State of Arizona Technology & Research Initiative Funding Photonics Foundation.

References

1. J. Chilla, S. Butterworth, A. Zeitschel, J. Charles, A. Caprara, M. Reed, and L. Spinelli, *Proc. SPIE* **5332**, 143 (2004).
2. L. Fan, M. Fallahi, A. Zakharian, J. Hader, J. Moloney, R. Bedford, J. Murray, W. Stolz, and S. Koch, *IEEE Photon. Technol. Lett.* **19**, 544 (2007).
3. T.-L. Wang, Y. Kaneda, M. Yarborough, J. Hader, J. Moloney, A. Chernikov, S. Chatterjee, S. Koch, B. Kunert, and W. Stolz, *IEEE Photon. Technol. Lett.* **22**, 661 (2010).
4. A. Bloom, *J. Opt. Soc. Am.* **64**, 447 (1974).
5. J. Hopkins, A. Maclean, D. Burns, E. Riis, N. Schulz, M. Rattunde, C. Manz, K. Köhler, and J. Wagner, *Opt. Express* **15**, 8212 (2007).
6. T. Leinonen, Y. A. Morozov, A. Harkonen, and M. Pessa, *IEEE Photon. Technol. Lett.* **17**, 2508 (2005).
7. G. Baili, L. Morvan, M. Alouini, D. Dolfi, F. Bretenaker, I. Sagnes, and A. Garnache, *Opt. Lett.* **34**, 3421 (2009).
8. V. Pal, P. Trofimoff, B.-X. Miranda, G. Baili, M. Alouini, L. Morvan, D. Dolfi, F. Goldfarb, I. Sagnes, R. Ghosh, and F. Bretenaker, *Opt. Express* **18**, 5008 (2010).
9. H. G. Winful and S. S. Wang, *Appl. Phys. Lett.* **53**, 1894 (1988).
10. M. Möller, B. Forsmann, and W. Lange, *Chaos Solitons Fractals* **10**, 825 (1999).
11. S. Corzine, R. Geels, J. Scott, R. H. Yan, and L. Coldren, *IEEE J. Quantum Electron.* **25**, 1513 (1989).
12. M. Raja, S. Brueck, M. Osinski, C. Schaus, J. McInerney, T. Brennan, and B. Hammons, *IEEE J. Quantum Electron.* **25**, 1500 (1989).
13. M. Walton, N. Terry, J. Hader, J. Moloney, and R. Bedford, *Appl. Phys. Lett.* **95**, 111101 (2009).
14. L. Coldren and S. Corzine, *Diode Lasers and Photonic Integrated Circuits* (Wiley, 1995).
15. SimuLase Version 1.4.0.0 by Nonlinear Control Strategies, Inc. (2009).
16. A. Siegman, *Lasers* (University Science, 1986).